Available online at www.sciencedirect.com

Journal of Catalysis 229 (2005) 490–498

JOURNAL OF CATALYSIS

www.elsevier.com/locate/jcat

Effect of the matrix in niobium-based aerogel catalysts for the selective oxidation of olefins with hydrogen peroxide

Filippo Somma [a], Patrizia Canton [b], Giorgio Strukul [a,*]

[a] *Dipartimento di Chimica, Università di Venezia, and Consorzio INSTM, Dorsoduro 2137, 30123 Venezia, Italy*
[b] *Dipartimento di Chimica Fisica, Università di Venezia, and Consorzio INSTM, Dorsoduro 2137, 30123 Venezia, Italy*

Received 21 July 2004; revised 16 November 2004; accepted 24 November 2004

Abstract

The preparation of a series of niobium-based aerogel samples under acidic and basic conditions is reported. The effect of the matrix (SiO_2, Al_2O_3, ZrO_2) and of the gelation conditions (acidic or basic) on the surface area, the porosity, and the catalytic activity of the solids in the oxidation of different substrates with hydrogen peroxide is investigated. The amount of niobium is constant in all samples.

The oxidation of unsubstituted (cyclooctene) and substituted (geraniol, nerol, and trans-2-pentene-1-ol) olefins is studied. The catalysts are moderately active but produce epoxides in good yields. The latter are influenced by the matrix properties (surface acidity and surface area). The preparation method makes it possible to prepare catalysts that are resistant to leaching and can be recycled several times without appreciable loss of activity.

Keywords: Oxidation; Olefins; Hydrogen peroxide; Sol–gel; Nb_2O_5 catalysts

1. Introduction

The synthesis of transition metal-containing catalysts active in selective oxidation reactions is an area of growing interest in catalysis. Titanium-based catalysts have been the most successful and thoroughly studied systems that have proved stable and active in oxidation reactions with hydrogen peroxide and alkyl hydroperoxides [1]. Recently other metals with redox properties such as Zr [2], W [3,4], V [5], and Mo [4] have been incorporated into mixed-metal oxides and used in these catalytic reactions. Two fundamental requirements for good catalytic performance and high stability are high dispersion of the catalytically active component within the matrix (site isolation) and stability to leaching [6]. Recently Ziolek et al. reported that Nb-containing molecular sieves can be as active and stable as V- and Ti-containing homologues [7]. These authors found that niobium-based catalysts show potential applications in different reactions such as NO decomposition, NO reduction, oligomerization, oxidative dehydrogenation of alkanes, and the oxidation of olefins with hydrogen peroxide. In these catalysts MCM-41 is most commonly used as a support. In this case, incorporation of Nb into the matrix framework determines the formation of defects that are important in the overall catalytic behavior of these materials. To date, modification of the catalytic activity in oxidation reactions by niobium oxides when these are incorporated into different matrixes has not been investigated in much detail.

In oxidation catalysts, such as VO_x-based catalysts, the support plays an important role in the performance of the catalyst [8]. The differences in behavior have been attributed to modifications in the nature of the interaction with the support. Supported niobia catalysts dispersed on high-surface area Al_2O_3, SiO_2, ZrO_2, and TiO_2 have already shown significant activity in the selective catalytic reduction of NO_x with NH_3, and Nb_2O_5–SiO_2 exhibited good selectivity in the oxidation of methanol to formaldehyde [9]. In this case, the matrix exerted a strong influence on the acidity of the mate-

---

[*] Corresponding author. Fax +39 041 234 8517.
E-mail address: strukul@unive.it (G. Strukul).

0021-9517/$ – see front matter © 2004 Elsevier Inc. All rights reserved.
doi:10.1016/j.jcat.2004.11.028

rial and on the coordination geometry of the niobia surface species [10].

Therefore, we thought it would be interesting to study the influence of the matrix in niobium-based mixed oxide catalysts for the oxidation of olefins with hydrogen peroxide, a reaction that has not been considered in much detail in the past [7]. In this work we describe the preparation by aerogel techniques and the characterization of a series of niobia mixed oxides dispersed on SiO_2, Al_2O_3, and ZrO_2 and their use as catalysts in the oxidation of simple (cyclooctene) and functionalized (geraniol, nerol, and *trans*-2-pentene-1-ol) olefins with hydrogen peroxide.

2. Experimental

2.1. Materials

The following metal alkoxides were used: tetramethoxysilane (TMOS) (Aldrich), tributoxyaluminum, and tetrapropoxyzirconium (Fluka). Other starting materials were niobium chloride (Aldrich); isopropanol, ethanol, and ammonia (BDH); and nitric acid and acetylacetone (Fluka). The oxidant was 35% hydrogen peroxide (Fluka). Substrates and solvent (methanol) were purchased from Fluka. All chemicals were purum or puriss grade and were used without further treatment.

2.2. Methods

BET surface areas and pore size were determined with N_2 at 77 K on a Micromeritics ASAP 2000 apparatus. X-ray powder diffraction analysis was performed with an X'Pert diffractometer operating with Cu-Kα Ni-filtered radiation, a graphite monochromator, and a proportional counter with a pulse height discriminator. The diffraction patterns were measured step by step (0.05° in 2θ).

GC-MS measurements were performed on a Hewlett–Packard 5971 mass selective detector connected to a Hewlett–Packard 5890 II gas chromatograph.

2.3. Synthesis of $Nb(OPr)_5$

Sodium (0.25 g) was dissolved in 50 ml of anhydrous isopropanol under a N_2 atmosphere with vigorous stirring. When complete dissolution was attained, 0.586 g of $NbCl_5$ was added to the solution and the mixture was stirred for 90 min. A clear solution of $Nb(OPr)_5$ in isopropanol was separate by centrifugation and brought to dryness in vacuo, and the obtained solid was dissolved in 20 ml of isopropanol.

2.4. Preparation of aerogels under acid conditions

A modified niobium alkoxide precursor was synthesized according to the procedure reported in Ref. [11].

In a typical procedure, a solution of acetylacetone (acacH, 45 µl), i-PrOH (3 ml), and $Nb(OR)_5$ (1.97 ml acac/$Nb(OR)_5$ 2/1 molar ratio) was heated under reflux for 1 h under N_2 with stirring. The modified niobium precursor and the support precursor (TMOS 9.8 ml) were dissolved in i-PrOH (10 ml). A hydrolyzing solution consisting of distilled water (6 ml) and nitric acid (0.27 ml) diluted in i-PrOH (6 ml) was added dropwise to the alkoxide solution under vigorous stirring. After 90 min, 40 ml i-PrOH was introduced into the system. The H_2O/alkoxide/acid molar ratio obtained was 5:1:0.09. In the Si-containing sample no gelation was observed. The mixture was transferred to a stainless-steel autoclave for solvent evaporation.

In the synthesis of Al_2O_3- and ZrO_2-based samples the molar ratios of the different reagents (alkoxides, water, isopropanol, and nitric acid) were kept constant and identical to those reported above ($Zr(O{-}i{-}Pr)_4$ 14.4 ml; $Al(O{-}Bu)_3$ 20.1 ml), whereas differences in volume were compensated for with isopropanol. In these cases a large amount of a white precipitate is formed with the addition of the hydrolizing solution. The mixtures were transferred to a stainless-steel autoclave for solvent evaporation.

The samples prepared with this procedure are denoted Nb_2O_5–SiO_2(a), Nb_2O_5–Al_2O_3, and Nb_2O_5–ZrO_2.

2.5. Preparation of the aerogel under basic conditions

Ethanol (25 ml) and 2.1 ml of NH_3 were added to the modified niobium precursor and TMOS (9.8 ml) solution under vigorous stirring. After 90 min, 60 ml i-PrOH was introduced to the system. Hydrolysis occurred within 5 min. The mixture was transferred to a stainless-steel autoclave for solvent evaporation.

The sample prepared with this procedure is denoted Nb_2O_5–SiO_2(b).

2.6. Evaporation of the solvent

The conditions for obtaining a supercritical evaporation of the solvent are $V_c = 48$ ml, $P_c = 48$ atm, $T_c = 235\,°C$. The high-pressure system was flushed with N_2, pressurized to 7 atm, and heated at 240 °C. The autoclave was kept at a final temperature for 60 min to ensure complete thermal equilibration. The final pressure was about 80 atm. The pressure was then released at constant temperature, and finally the system was flushed with N_2 and cooled down to room temperature. All samples were calcined at 500 °C in air for 150 min (gas flow 30 ml/min; heating ramp 3 °C/min).

2.7. TPD of pyridine

The thermally programmed desorption (TPD) of pyridine was employed for the determination of the acid sites [12]. A sample of the calcined catalyst (5 mg) was activated in air flow (30 ml/min) at 500 °C for 60 min, cooled to RT, and saturated for 5 min with a stream of pyridine coming from saturator kept at RT. The sample was then purged with He (25 ml/min) at 100 °C. The temperature was cooled to 40 °C, and then the TPD was started (heating ramp 10 °C/min, maximum temperature 400 °C). The desorption of pyridine was monitored by a FID detector connected online.

2.8. Catalytic oxidation procedures

Catalytic reactions were performed in 10-ml glass vials equipped with a condenser and a small magnetic bar. The catalyst (30 mg), substrate (2 mmol), solvent (methanol, 1 ml), and H_2O_2 (1 mmol) were placed in the vial under N_2 flow. The reaction vessels were sealed and placed in an oil bath at constant temperature (70 and 90 °C), and an external magnetic stirrer ensured agitation. At different reaction times the vials were cooled to room temperature, and the corresponding reaction mixtures were analyzed by GC. Product identification was performed by GC-MS analysis and by comparison with authentic samples. Residual H_2O_2 was determined by iodometric titration.

3. Results and discussion

3.1. Preparation

To check the effect of the matrix on the behavior of niobium in the oxidation reactions considered, matrixes with different characteristics were chosen, namely, (i) SiO_2, a high-surface-area, relatively inert material, prepared both under acid and basic conditions; (ii) Al_2O_3, a medium-surface-area material with amphoteric properties [13], generally capable of interacting with the active phase; (iii) ZrO_2, a transition-metal oxide, generally of medium-low surface area. Since all of the prepared mixed oxides were made of elements of different valences, acidic properties were expected in all samples.

All aerogels were prepared via sol–gel methods. Under the conditions reported in Section 2, gelation for the Nb_2O_5–SiO_2(b) sample, which was synthesized under basic conditions, occurs in 4–5 min, and a colorless gel is obtained. The homologous sample obtained under acidic conditions did not show any apparent gelation. In this case, the supercritical evaporation of the solvent is a fundamental step for obtaining a transparent gel. In the case of the Al_2O_3- and ZrO_2-based samples, the acidic conditions led to the formation of a large amount of white gel with the addition of the hydrolyzing solution.

All gels were aged in air for 20 h. They were subsequently dried in an autoclave. Finally, samples were calcined at 500 °C for 150 min in air flow. They all contained 0.5% Nb.

3.2. Characterization

X-ray powder diffraction (Fig. 1A) analysis of the different catalysts indicated no niobia was detected in any sample, which is a reasonable indication that no Nb_2O_5 segregation occurs during the preparation procedure and Nb is well dispersed in the respective oxide matrix [14]. Fig. 1A shows the typical X-ray diffraction patterns of amorphous SiO_2 and indicates the presence of the typical features of γ-Al_2O_3 and tetragonal/monoclinic ZrO_2. In principle, the low Nb amount (0.5 wt%) is not a limitation to detection, since the XRD pattern (Fig. 1B) of a 0.5 wt% Nb-containing mechanical mixture of Nb_2O_5 in silica shows clearly the two most intense peaks at 22.76 and 36.67 typical of hexagonal niobia.

Surface area and pore size distribution were determined from N_2 adsorption/desorption isotherms; some typical ones are shown in Fig. 2A. A summary of the morphological properties of the different samples is given in Table 1.

In general, the aerogels showed a type III isotherm with a type H1 desorption hysteresis loop [15]. Table 1 indicates that relatively large surface areas can be obtained for all samples as a consequence of the aerogel preparation method. As expected, the surface area is larger for the SiO_2-

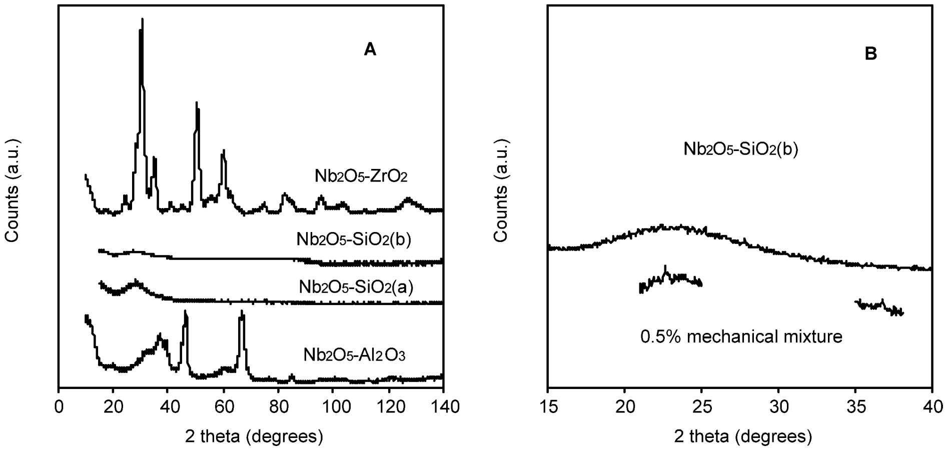

Fig. 1. (A) Powder X-ray diffraction analysis of the different Nb containing catalysts. (B) Comparison between Nb_2O_5–SiO_2(b) and a 0.5 wt% Nb containing mechanical mixture of Nb_2O_5 in silica showing the two most intense peaks at 22.76 and 36.67 typical of hexagonal niobia.

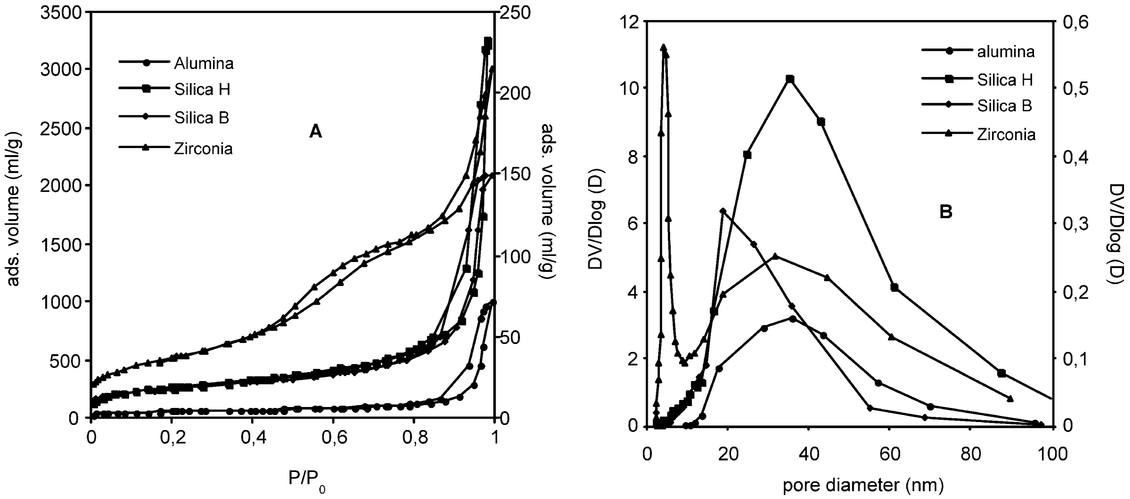

Fig. 2. (A) BET adsorption isotherms and (B), BJH poresize distribution of the different Nb containing catalysts. In both cases the zirconia containing sample refers to the y axis on the right hand side.

Table 1
Morphological properties of the different niobium containing samples

Sample	Surface area BET (m^2/g)	Pore distribution maxima (nm)	Pore volume (ml/g)
Nb_2O_5–SiO_2(a)	940	35	5.04
Nb_2O_5–SiO_2(b)	916	19	3.24
Nb_2O_5–Al_2O_3	197	36	1.54
Nb_2O_5–ZrO_2	133	4, 32[a]	0.33

[a] Bimodal distribution.

based catalysts and decreases in the order Nb_2O_5–SiO_2(a) $\sim$ Nb_2O_5–SiO_2(b) $>$ Nb_2O_5–Al_2O_3 $>$ Nb_2O_5–ZrO_2. The pore size distribution, derived from the desorption branch of the isotherm, shows a large, unimodal distribution in the range of large mesopores (maxima in the 18–36-nm range) for all samples. The only exception is Nb_2O_5–ZrO_2 (Fig. 2B), for which a bimodal distribution is observed (maxima at 4 nm and at 32 nm). For this sample a double hysteresis loop is quite evident in Fig. 2A. The pore volume increased in the order Nb_2O_5–SiO_2(a) $>$ Nb_2O_5–SiO_2(b) $\gg$ Nb_2O_5–Al_2O_3 $>$ Nb_2O_5–ZrO_2.

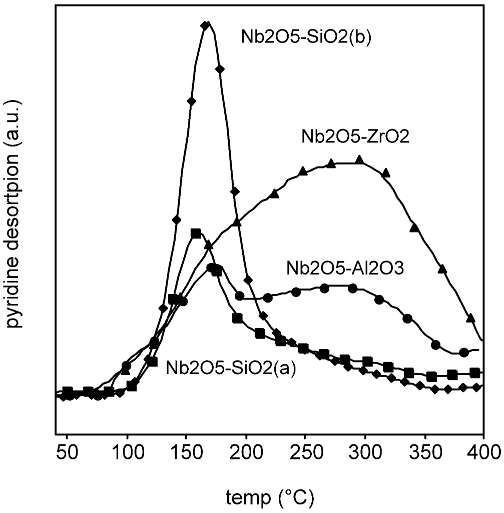

Fig. 3. Pyridine TPD profiles of the different Nb containing catalysts.

Table 2
Acid site dosage determined by pyridine TPD experiments (Fig. 3)

Sample	Pyridine relative amount (a.u.)	160 °C acid sites (a.u.)	200 °C acid sites (a.u.)	280 °C acid sites (a.u.)
Nb_2O_5–SiO_2(a)	26	6	20	
Nb_2O_5–SiO_2(b)	52	33	19	
Nb_2O_5–Al_2O_3	41	8		33
Nb_2O_5–ZrO_2	100	3		97

3.3. *Acidity measurements*

A general characterization of the acidity properties of the catalyst surface was made by pyridine desorption. Fig. 3 shows the pyridine TPD profiles of the different catalysts, from which the presence of different amounts and different types of acid sites can be inferred. As can be seen, two bands are evident in all samples. A deconvolution of the different curves made it possible to resolve the different components: a low-temperature one at 160–170 °C, present in all samples, indicative of relatively weak acid sites; another one at 200–210 °C, present only in the silica-based samples, indicative of medium acid sites; and finally one at 280–290 °C, present in Nb_2O_5–Al_2O_3 and Nb_2O_5–ZrO_2, indicative of stronger acid sites. The relative amounts of the total acid sites and the contribution of the individual components in the catalyst samples are reported in Table 2. With respect to the total amount of pyridine adsorbed, the samples show the acidity order Nb_2O_5–ZrO_2 $\gg$ Nb_2O_5–SiO_2(b) $>$ Nb_2O_5–Al_2O_3 $>$ Nb_2O_5–SiO_2(a), however, whereas the two silica-based samples possess only weak or moderate acid sites, in the case of Nb_2O_5–ZrO_2 and Nb_2O_5–Al_2O_3 the acidity is mainly due to strong sites (see Table 2).

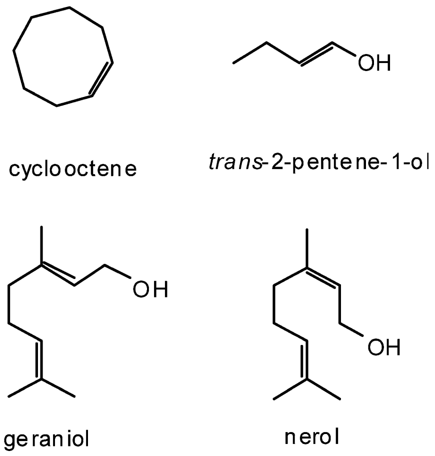

Chart 1.

3.4. Oxidation of cyclooctene

The oxidation of cyclooctene (Chart 1) with 35% hydrogen peroxide was chosen as the reference reaction to compare the behavior of the different catalysts. Cyclooctene is an interesting test reagent because of the high stability of the corresponding epoxide. Reactions were carried out in methanol, a solvent that is commonly preferred for industrial applications, as it is cheap and completely miscible with hydrogen peroxide. In a previous report on the epoxidation of cyclohexene, other authors [7,16] have found that the use of acetonitrile as the solvent is very important for maximizing selectivity for epoxide, whereas in methanol the reaction gave almost exclusively glycol. Indeed, acetonitrile can add H_2O_2 under basic conditions to form peroxycarboximidic acid, which is able to convert alkenes into epoxides without any catalyst [17], so its use may be misleading. On the other hand, protic media, such as methanol, have been recognized to increase the electrophilicity of the metal center (hence its Lewis acidity) in, for example, Ti-containing zeolites as catalysts [18]. For this reason and because of the results reported below, methanol was the solvent of choice.

Some typical reaction profiles obtained with the individual catalysts are shown in Fig. 4, and a summary of the conversions of cyclooctene and hydrogen peroxide is given in Table 3. Cyclooctene epoxide was the only product observed. In Table 3, a comparison between methanol and acetonitrile, made with the use of the two Nb_2O_5–SiO_2 catalysts, is also presented. As can be seen, the latter solvent is a poorer reaction medium, leading to lower epoxide formation and higher hydrogen peroxide consumption.

Fig. 4 shows that at 70 °C the reaction is virtually finished after about 150–200 min with all catalysts except Nb_2O_5–SiO_2(a), which is still active even after 300 min. Notably, the use of an identical amount of a homogeneous complex such as $Nb(OPr)_5$, the precursor used for the preparation of the catalysts, seems to lead to a better conversion with respect to the mixed-oxide catalysts. This result was somehow unexpected, as Ziolek and co-workers [7], in studying the possible effect of Nb leaching from NbMCM-41, found that Nb oxalate (i.e., the precursor used in their preparation) was completely inactive in the epoxidation of cyclohexene. Indeed, Nb oxalate is a rather thermally unstable species, and its formation as a leached species from NbMCM-41 calcined at 550 °C seems unlikely under catalysis conditions; a solvent (acetonitrile) or hydroxy species appears to be a more likely form of dissolution of Nb.

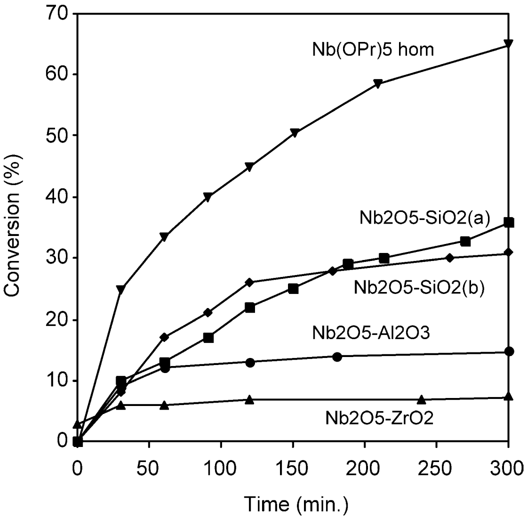

Fig. 4. Conversion vs time plots of the epoxidation of cyclooctene with hydrogen peroxide, using different Nb containing catalysts.

Table 3
Oxidation of cyclooctene with hydrogen peroxide catalyzed by different niobium containing catalysts[a]

Catalyst	Temperature (°C)	Conversion (%)	
		Cyclooctene	H_2O_2
Nb_2O_5–SiO_2(a)	70	36	65
Nb_2O_5–SiO_2(b)	70	31	66
Nb_2O_5–SiO_2(a)[b]	70	10	85
Nb_2O_5–SiO_2(b)[b]	70	16	85
Nb_2O_5–Al_2O_3	70	15	46
Nb_2O_5–ZrO_2	70	8	100
Nb_2O_5–SiO_2(a)	90	61	71
Nb_2O_5–SiO_2(b)	90	25	93
Nb_2O_5–Al_2O_3	90	13	39
Nb_2O_5–ZrO_2	90	8	95

[a] Experimental conditions: catalyst, 30 mg; substrate, 2 mmol; 35% H_2O_2, 1 mmol; reaction time, 5 h.

[b] Reactions carried out in acetonitrile instead of methanol.

Fig. 4 and Table 3 indicate that the two silica-based samples are the best catalysts for the epoxidation reaction, and zirconia is the worst support, as it leads to extensive decomposition of hydrogen peroxide with very little epoxide productivity, in agreement with some previous observations [14]. The efficiency in the use of hydrogen peroxide, that is, the amount that goes into epoxide, is about 50% or less. To improve this efficiency we also tested a different way to feed the oxidant to the reaction mixture. As explained in Section 2, H_2O_2 is generally added to the system all in one shot. Parallel experiments were carried out with Nb_2O_5–SiO_2(a) and Nb_2O_5–SiO_2(b), in which the amount

Table 4
Effect of the introduction of the oxidant in different aliquots on the conversions of cyclooctene and hydrogen peroxide[a]

Sample	Reaction time (h)	Cyclooctene (%)	H_2O_2 (%)
Nb_2O_5–SiO_2(a)	5	32	35
	22	100	100
Nb_2O_5–SiO_2(b)	5	35	65
	22	62	100

[a] Experimental conditions: catalyst, 30 mg; substrate, 2 mmol; 35% H_2O_2 (total), 1 mmol; temperature, 70 °C.

of hydrogen peroxide was divided into nine aliquots that were fed to the system every 30 min. This helps to keep the concentration of H_2O_2 in the system low and should limit side decomposition reactions. The results of these experiments are collected in Table 4. As can be seen, only with Nb_2O_5–SiO_2(a) does this stepwise mode of feeding hydrogen peroxide lead to a significant improvement in cyclooctene conversion and hydrogen peroxide efficiency. Notably, full conversion is observed after 22 h. Conversely, a comparison between Tables 4 and 3 indicates that the use of Nb_2O_5–SiO_2(b) seems to be unaffected by the different H_2O_2 feeding procedure.

To improve the conversions the reaction temperature was increased to 90 °C. Again (Table 3), this seems to be beneficial only for Nb_2O_5–SiO_2(a), which leads to an excellent balance between the conversions of epoxide (61%) and hydrogen peroxide (71%), indicating that only a small fraction of the latter is decomposed under the experimental conditions used.

3.5. Catalyst recycling

Catalyst recycling tests were carried out for all samples. The oxidation of cyclooctene was tested with fresh samples, followed by a series of recycling with the solids isolated by filtration from the previous reaction mixture. The recovered solids were always dried for 20 h in the oven at 110 °C and reused. After the third cycle the samples were calcined at 500 °C. A summary of the results obtained in the different cycles is collected in Table 5. As can be seen, after four cycles there is no loss of activity (conversion) and the consumption of hydrogen peroxide remains the same. It must be emphasized that the solutions separated from each a reaction mixture were completely inactive when fresh oxidant and substrate were added. In view of the good homogeneous catalytic activity observed for $Nb(OPr)_5$, this observation strongly supports the heterogeneous character of the present catalysts.

Interestingly, in the case of Nb_2O_5–SiO_2(a) the calcination at 500 °C after the third cycle leads to some improvement in both epoxide formation and hydrogen peroxide consumption.

In summary, after this series of experiments on the epoxidation of cyclooctene, Nb_2O_5–SiO_2(a) appears to be the most interesting catalyst in terms of both activity and selectivity for the use of hydrogen peroxide and the possibility of recycling.

Table 5
Effect of catalyst recycling in the oxidation of cyclooctene with hydrogen peroxide catalyzed by different niobium containing catalysts[a]

Recycle	Catalyst	Cyclooctene conversion (%)	Time (min)	H_2O_2 conversion (%)
Fresh	Nb_2O_5–SiO_2(a)	35	300	64
	Nb_2O_5–SiO_2(b)	31	255	66
	Nb_2O_5–Al_2O_3	17	60	48
	Nb_2O_5–ZrO_2	7	30	100
1st	Nb_2O_5–SiO_2(a)	34	300	68
	Nb_2O_5–SiO_2(b)	36	240	60
	Nb_2O_5–Al_2O_3	9	244	36
	Nb_2O_5–ZrO_2	11	40	100
2nd	Nb_2O_5–SiO_2(a)	39	300	65
	Nb_2O_5–SiO_2(b)	34	227	64
	Nb_2O_5–Al_2O_3	8	200	36
	Nb_2O_5–ZrO_2	10	30	100
3rd after calcination at 500 °C	Nb_2O_5–SiO_2(a)	46	265	60
	Nb_2O_5–SiO_2(b)	35	254	62
	Nb_2O_5–Al_2O_3	9	208	35

[a] Experimental conditions: catalyst, 30 mg; substrate, 2 mmol; 35% H_2O_2, 1 mmol; temperature, 70 °C; reaction time, 5 h.

3.6. Oxidation of allylic alcohols

The oxidation of cyclooctene, in view of the stability of the corresponding epoxide, does not allow us to address selectivity issues related to the different acidities of the catalysts. For this reason three allylic alcohols, namely geraniol, nerol, and *trans*-2-penten-1-ol (see Chart 1), were tested in the oxidation with hydrogen peroxide. Geraniol and nerol show interesting properties, as they have two different double bonds: one is in the allylic position with respect to the –OH group, and the other one (the 6–7 double bond) is isolated. In principle, different epoxidation products can be observed, all giving the corresponding diols upon hydrolysis. In all cases we have observed only the oxidation of the 2–3 double bond with the formation of the corresponding epoxyalcohol, and the subsequent ring opening due to hydrolysis and formation of the corresponding diol (actually a triol). This behavior is typical for tungsten and titanium chemistry [19,20], where the –OH functionality is known to coordinate to the transition metal center and olefin epoxidation occurs preferentially at the allylic position.

The reaction was carried out in the presence of methanol as the solvent and in the same conditions as used for the epoxidation of cyclooctene. Fig. 5 shows the profiles of conversion (A) and selectivity (B) versus time in the oxidation of geraniol. As can be seen, silica-based catalysts (Fig. 5A) show much better activity with respect to Nb_2O_5–Al_2O_3 and Nb_2O_5–ZrO_2. In particular, the catalyst giving the best performance is Nb_2O_5–SiO_2(b), in terms of both activity

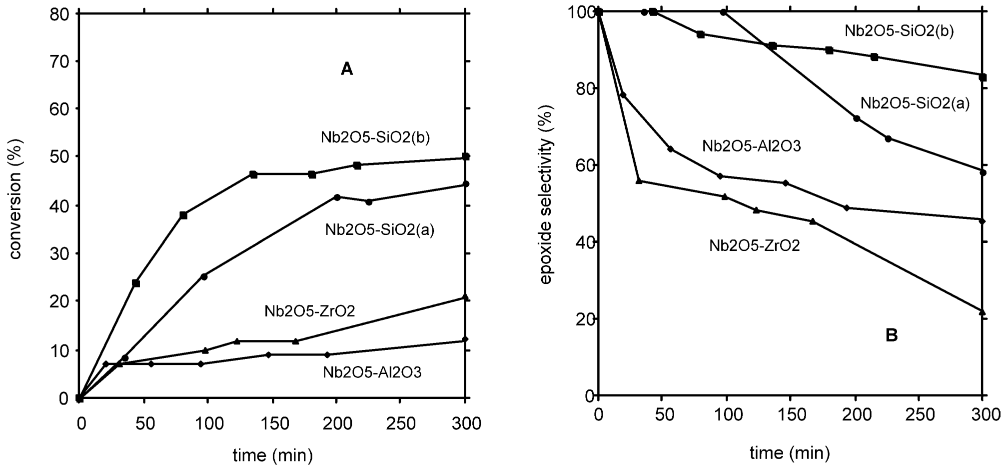

Fig. 5. (A) conversion vs time plots and (B), selectivity to epoxide vs time plots for the oxidation of geraniol using different Nb containing catalysts.

and selectivity. The latter parameter refers to epoxide versus diol, as no other oxidation products were observed. Fig. 5B clearly indicates that the two silica-based samples maintain 100% selectivity for epoxide for about 50–100 min, then, as the concentration of epoxide in the system increases, the selectivity decreases with the formation of diols. In the case of Nb_2O_5–SiO_2(b) it remains relatively stable in the range of 85–90%, whereas with Nb_2O_5–SiO_2(a) it drops quite significantly to less than 60%. The case of Nb_2O_5–Al_2O_3 and Nb_2O_5–ZrO_2 is quite different. Their conversions are poor and their selectivities for epoxide drop dramatically from the beginning of the reaction. In particular, in the case of Nb_2O_5–ZrO_2 the selectivity for epoxide drops to a poor 20% after a reaction time of 5 h. This behavior, on the one hand, reflects the high content of strong acid sites evidenced by pyridine desorption (Table 2) observed with alumina and zirconia supports, but on the other hand it seems to suggest that hydrolysis occurs on the silica-supported samples with a different mechanism with respect to the alumina/zirconia samples. We tentatively suggest that with the former supports the epoxide is probably rapidly desorbed and is hydrolyzed by readsorption on the acid sites, only after a certain concentration is established in solution (approximately 25–30% conversion). With the latter supports hydrolysis probably occurs mainly on site without desorption of the epoxide.

The general trend that emerges from Fig. 5B is that all acid sites are capable of hydrolyzing the oxirane ring; however, weak or medium-strength acid sites make it possible to maintain a fair selectivity for epoxide.

A summary of the results obtained with the different substrates is reported in Table 6. Again, selectivity refers to epoxide versus diol, as no other oxidation products were observed. The general observations on the activity obtained from Fig. 5A for geraniol apply to all substrates reported (see in Fig. 6A the conversion versus time curves for nerol). Indeed, with *trans*-2-penten-1-ol both Nb_2O_5–Al_2O_3 and Nb_2O_5–ZrO_2 were found to be inactive. What is intriguing is the selectivity observed with the different catalysts in the case of nerol (Fig. 6B). With this substrate, the selectivity ranking is approximately the same as with geraniol. However the selectivities are in general much better, and all catalysts seem to follow an epoxide desorption–readsorption mechanism prior to hydrolysis. The difference between strong and weak acid sites that seemed to justify the results obtained with geraniol appears to be more elusive in this case.

Table 6
Oxidation of different allylic alcohols with hydrogen peroxide catalyzed by different niobium containing catalysts[a]

Substrate	Sample	Substrate conversion (%)	Epoxide selectivity (%)	H_2O_2 conversion (%)
Geraniol	Nb_2O_5–SiO_2(a)	44	58	90
	Nb_2O_5–SiO_2(b)	50	83	95
	Nb_2O_5–Al_2O_3	12	45	65
	Nb_2O_5–ZrO_2	21	22	95
Nerol	Nb_2O_5–SiO_2(a)	46	86	93
	Nb_2O_5–SiO_2(b)	65	83	100
	Nb_2O_5–Al_2O_3	20	77	40
	Nb_2O_5–ZrO_2	11	70	100
trans-2-Penten-1-ol	Nb_2O_5–SiO_2(a)	36	84	60
	Nb_2O_5–SiO_2(b)	39	95	85
	Nb_2O_5–Al_2O_3	0		45
	Nb_2O_5–ZrO_2	0		95

[a] Experimental conditions: catalyst, 30 mg; substrate, 2 mmol; 35% H_2O_2, 1 mmol; temperature, 70 °C; reaction time, 5 h.

3.7. Stereochemical and mechanistic considerations

The reason for this different behavior relies most likely on the different geometries of the two epoxides. In fact, similar to what was observed with previously reported WO_3–SiO_2 mixed oxide catalysts [20], these epoxidation reactions are stereoselective, in the sense that the *trans* olefin (geraniol) gives the *trans* epoxide, whereas the *cis* olefin (nerol) gives the *cis* epoxide. The latter is sterically more hindered than the former, and this might explain why it desorbs more quickly from the active site.

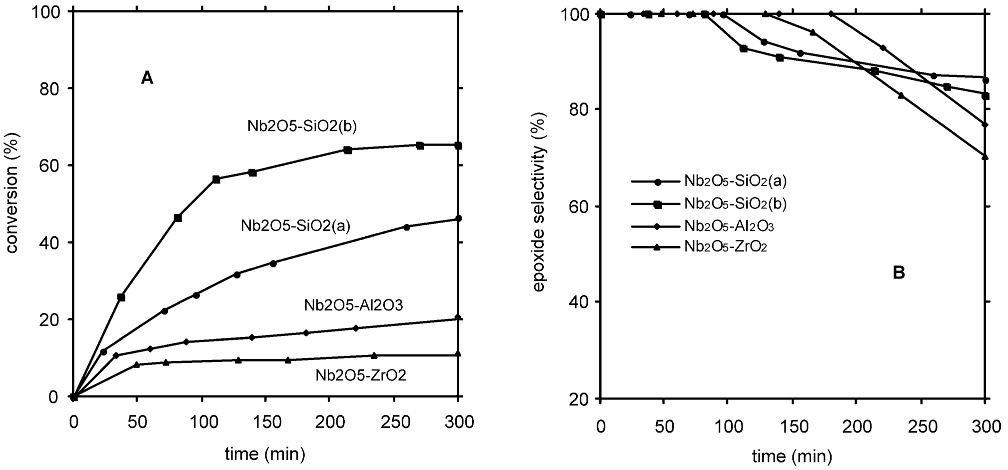

Fig. 6. (A) conversion vs time plots and (B), selectivity to epoxide vs time plots for the oxidation of nerol using different Nb containing catalysts.

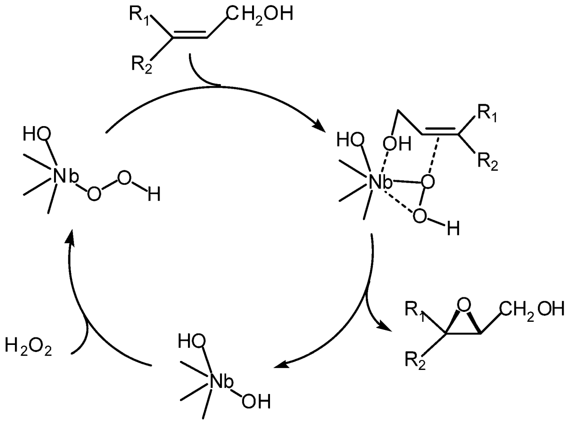

Scheme 1.

The oxidation occurring exclusively at the allylic C=C double bond observed with the present catalysts, the stereochemical correlation between allylic alcohols and epoxides, and the possibility of catalyst recycling reported in Table 5 seem to suggest for the oxygen transfer step a mechanism similar to the one suggested by Kumar et al. [20] for the epoxidation of geraniol with hydrogen peroxide catalyzed by TS-1, shown in Scheme 1. The mechanism is very similar to the classic one suggested by Sharpless for soluble species [21] and consists of (i) the activation of the oxidant at the metal center, (ii) the pivotal role of the allylic alcoholic function in bringing the C=C double bond close to the peroxy oxygen, and (iii) the concerted transfer of oxygen via the so-called butterfly transition state, which is responsible for the stereochemistry of the epoxide.

4. Conclusions

The results reported in this work clearly show that aerogel preparation methods are a viable way to prepare large-pore niobia mixed oxides dispersed on different supports with controlled morphological properties. These samples are indeed effective catalysts for the selective oxidation of simple olefins and allylic alcohols with hydrogen peroxide to give the corresponding epoxides. Reactions can be conveniently carried out in solvents such as methanol, and this may be attractive for practical use.

The major effect exerted by the different oxides when mixed with niobia is the generation of acid sites of different strengths that can have a major influence on the activity and selectivity toward the different substrates and on the decomposition of the oxidant and hence on the efficiency with which the latter is employed in the reaction. In this respect, the mode of feeding hydrogen peroxide to the system can have a strong influence. In fact, a stepwise addition can lead to 100% efficiency. Silica-based catalysts are by far the most active and selective.

Catalysts can be recycled several times with no loss of activity and some benefits with respect to epoxide selectivity. These properties are related to the preparation method, which allows the formation of amorphous Nb_2O_5 entities that are well dispersed and tightly held within the matrix. This ensures the formation of materials that are very stable against leaching and sintering under catalytic conditions.

Finally, in the case of allylic alcohols, the regioselectivity of the reaction and the stereochemical correlation between the substrate and the product obtained make it possible to suggest an oxygen transfer pathway that is very similar to what has been known for more than 30 years from homogeneous catalysis.

Acknowledgments

We thank MIUR, Rome (PRIN 2003), and Consorzio INSTM, Firenze, for financial support for this work. We also express our gratitude to Dr. Michela Signoretto, Department of Chemistry, University of Venice, for many helpful discussions and suggestions.

References

[1] (a) B. Notari, Catal. Today 18 (1993) 63;
(b) M. Dusi, T. Mallat, A. Baiker, Catal. Rev. Sci. Eng. 42 (2000) 213.

[2] M. Morandin, R. Gavagnin, F. Pinna, G. Strukul, J. Catal. 212 (2002) 193.

[3] (a) R. Jin, H. Li, J. Deng, J. Catal. 203 (2001) 75;
(b) X. Xia, R. Jin, Y. He, J.-F. Deng, H. Li, Appl. Surf. Sci. 165 (2000) 255.

[4] R. Neumann, M. Levin-Elad, J. Catal. 166 (1997) 206.

[5] R. Neumann, M. Levin-Elad, Appl. Catal. A: General 122 (1995) 85.

[6] I.W.C.E. Arends, R.A. Sheldon, Appl. Catal. A: General 212 (2001) 175.

[7] (a) I. Nowak, B. Kilos, M. Ziolek, A. Lewandowska, Catal. Today 78 (2003) 487;
(b) M. Ziolek, Catal. Today 78 (2003) 47.

[8] M.L. Ferreira, M. Volpe, J. Mol. Cat. A: Chemical 164 (2000) 281.

[9] I.E. Wachs, J.M. Jehng, G. Deo, H. Hu, N. Arora, Catal. Today 8 (1990) 57.

[10] L.J. Burcham, J. Datka, I.E. Wachs, J. Phys. Chem. B 103 (1999) 6015.

[11] M. Aizawa, Y. Nosaka, N. Fujii, J. Non-Cryst. Solids 128 (1991) 77.

[12] (a) M. Skotak, Z. Karpinski, Chem. Eng. J. 90 (2002) 89;
(b) T. Kawai, K.M. Jiang, T. Ishikawa, J. Catal. 159 (1996) 288.

[13] J.C. Luyand, J.M. Parera, Appl. Catal. 26 (1986) 295.

[14] C. Palazzi, L. Oliva, M. Signoretto, G. Strukul, J. Catal. 194 (2000) 286.

[15] K.S.W. Sing, D.H. Everett, R.A. Haul, L. Moscou, R.A. Pierotti, J. Rouquerol, T. Siemieniewska, Pure Appl. Chem. 57 (1985) 603.

[16] B. Kilos, M. Aouine, I. Nowak, M. Ziolek, J.C. Volta, J. Catal. 224 (2004) 314.

[17] G.B. Payne, P.H. Deming, P.H. Williams, J. Org. Chem. 26 (1961) 659.

[18] (a) M.G. Clerici, P. Ingallina, J. Catal. 140 (1993) 71;
(b) V. Hulea, P. Moreau, J. Mol. Catal. A: Chemical 113 (1996) 499.

[19] D. Hoegaerts, B.F. Sels, D.E. de Vos, F. Verpoort, P.A. Jacobs, Catal. Today 60 (2000) 209.

[20] R. Kumar, G.C.G. Pais, B. Pandey, P. Kumar, Chem. Commun. 1315 (1995).

[21] K.B. Sharpless, J.M. Townsend, D.R. Williams, J. Am. Chem. Soc. 94 (1972) 295.